Colloid Polym Sci 280: 59–64 (2002)
© Springer-Verlag 2002

ORIGINAL CONTRIBUTION

Y. Fang
X. Zhu
D. Yan
Q. Lu
P. Zhu

Investigations on poly(ethylene oxide)–*p*-bromotoluene intercalate by in situ heating Fourier transform IR spectroscopy

Received: 5 March 2001
Accepted: 31 August 2001

Y. Fang · X. Zhu · D. Yan (✉)
College of Chemistry and Chemical Technology, Shanghai Jiao Tong University, Shanghai 200240, China
e-mail: dyyan@mail.sjtu.edu.cn
Fax: + 86-21-54741297

Q. Lu · P. Zhu
Instrumental Analysis Center
Shanghai Jiao Tong University
1954 Huashan Road
Shanghai 200030, China

Abstract By means of differential scanning calorimetry, the phase diagram of the poly(ethylene oxide)–*p*-bromotoluene system (PEO–PBT) is established. It is found that PEO and PBT form a molecular intercalate with a molar stoichiometry of 22%, which corresponds to two PBT molecules for seven ethylene oxide units. The intercalate undergoes an incongruent melting at 48.5 °C on heating. Wide-angle X-ray diffraction experiments indicate that the PEO–PBT intercalate has a crystalline structure different from pure PEO. From variable-temperature Fourier transform IR spectroscopy investigations, it is believed that the macromolecular chains in the PEO–PBT intercalate adopt a 7/2 helical conformation which is identical to that in the pure PEO. There are a considerably large number of helical structures in the melt of the PEO–PBT intercalate at temperatures ranging from 50 to 60 °C even though the crystalline lattices collapsed in the aforementioned temperature range. Such a kind of melt is in a conformationally high order state.

Keywords Poly(ethylene oxide) · Molecular intercalate · Phase diagram · Incongruent melting · Helical conformation

Introduction

It is known that poly(ethylene oxide) (PEO) can form crystalline complexes with a number of organic and inorganic molecules. In these crystalline complexes, the interactions between host and guest molecules can be classified into three cases:

1. Electrostatic interactions for inorganic salts ($HgCl_2$ [1], alkali salts [2], etc.).
2. Hydrogen bonds for urea [3], resorcinol [4, 5], *p*-nitrophenol [6], etc. In this category of complexes, hydrogen bonds between the oxygen ether of PEO chains and the hydroxyl group of guest molecules are so strong that the conformation of PEO chains changes largely and differs completely from that of pure PEO [7, 8]. Moreover, the crystal structures of these complexes vary from that of pure PEO.
3. van der Waals interactions for PEO–*p*-dihalogenobenzene (PEO–PD*X*) intercalates [9, 10]. As to these types of complexes, the interaction between the host PEO chains and the guest benzene halide molecules is relatively weak. The size and the shape of small guest molecules determine whether they can form crystalline intercalates with PEO or not. The weak van der Waals interactions in these complexes have little influence on the PEO chain conformation. Thus, the conformation of PEO chains changes slightly and adopts a 10/3 helix, which is very close to the 7/2 helix of pure PEO [11].

The existence of a PEO–*p*-bromotoluene (PEO–PBT) intercalate was first confirmed by Point et al. [10]; however, little attention has been paid to the phase diagram and chain conformation of the PEO–PBT intercalate. In contrast to PD*X*s, PBT interacts weakly with PEO because there is only one halogen atom in the molecule; therefore, it is possible that the thermal stability of the PEO–PBT intercalate is poorer than the PEO–PD*X* intercalates, and the macromolecular conformation is

different from the 10/3 helix adopted by PEO–PD*X* intercalates. In the present work, the PEO–PBT phase diagram is constructed from differential scanning calorimetry (DSC) data, and the chain conformation of the PEO–PBT intercalate is investigated using variable-temperature Fourier transform IR spectroscopy (FTIR).

Experimental

PEO with an average molecular weight of 6,000 was purchased from Shanghai Medicine and Chemical Reagent Corporation (China). PBT and *p*-dibromobenzene (PDBB) were analytical reagents and were used without further purification. The PEO–PDBB intercalate was prepared directly by four successive meltings and recrystallizations of stoichiometric mixtures of two components. The stoichiometry of the PEO–PDBB intercalate used in the preparation was 23% (i.e. three PDBB molecules for ten ethylene oxide units), which had been determined previously [9]. The phase transitions of the PEO–PBT systems were determined using a Pyris-1 series differential scanning calorimeter in a flowing nitrogen atmosphere. This instrument was calibrated by benzoic acid and indium. The scanning rate was 5 °C min^{-1}. About 5-mg mixtures of PEO and PBT were weighed into volatilization-proof aluminum caps. After being melted and recrystallized four times, the samples with good homogeneity were used for the determination of the phase transition.

The IR spectra were recorded at a resolution of 4.0 cm^{-1} using a Bruker Equinox-55 FTIR spectrometer equipped with a temperature-controllable cell. The samples used in the variable-temperature FTIR experiments were KBr pellets rather than films in order to avoid the orientation of the samples introduced by the method of film preparation [12]. The powder sample was pressed into a KBr pellet and then sandwiched between two thin NaCl plates. The sample was placed into the temperature-controllable cell and heated from 25 to 80 °C at 5 °C min^{-1}. At the same time, the FTIR spectra were recorded at a rate of one spectrum each 4 s, in order to obtain the relationship of the IR intensity with temperature. The peak height was chosen to evaluate the intensity of the IR band. The scanning wavenumber ranged from 4,000 to 400 cm^{-1}. It is worth mentioning that the KBr pellet should be pressed as thin as possible in order to avoid a temperature gradient.

The powder wide-angle X-ray diffraction (WAXD) spectra were obtained using a Rigaku Geiger Flex D-Max IIIa using Ni-filtered Cu Kα radiation (40 kV, 25 mA), and a scanning rate of 2° min^{-1} was applied.

Results and discussion

The PEO–PDBB phase diagram has been reported by Point et al. [9], and the stoichiometry of the PEO–PDBB intercalate is determined to be 23%; however, no study has been devoted to the determination of the PEO–PBT phase transition as yet. As a result, its stoichiometry has been uncertain. The partial phase diagram of the PEO–PBT systems obtained by the thermal analysis method is shown in Fig. 1. The phase diagram is characteristic of a peritectic system that has incongruent melting behavior. The presence of peritectic melting at 48.5 °C and eutectic melting at 24 °C confirms the formation of a molecular intercalate between PEO and PBT. Nevertheless the incongruent melting indicates the poor thermal stability

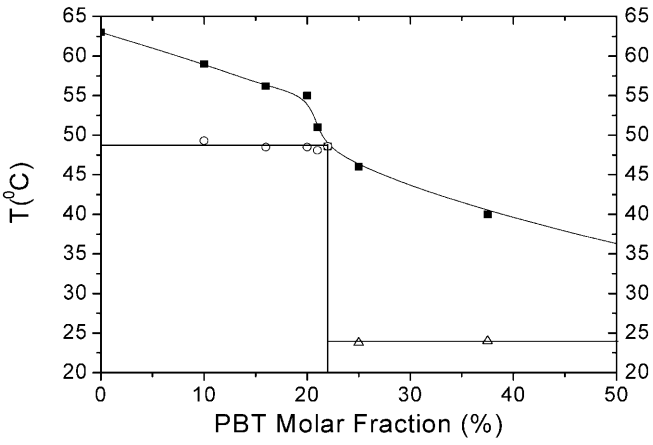

Fig. 1 The partial phase diagram of the poly(ethylene oxide) (*PEO*)–*p*-bromotoluene (*PBT*) system obtained from differential scanning calorimetry (*DSC*) data

of the PEO–PBT intercalate, which may be due to the very weak van der Waals interactions between PEO and PBT molecules. The phase diagram of the PEO–PBT system is similar to that of PEO–*p*-nitrophenol complex [8], but is different from that of the PEO–PDBB intercalate, which presents a bell-shaped domain [9]. The molar stoichiometry of the PEO–PBT intercalate is derived to be 22% by using the method suggested in Ref. [8], which corresponds to two PBT molecules for seven ethylene oxide units. It should be noted here that the stoichiometry of the PEO–PBT intercalate differs slightly from that of the PEO–PDBB intercalate.

Various melting curves obtained for the PEO–PDBB intercalate with a PDBB molar ratio of 23%, pure PEO and the PEO–PBT intercalate with a PBT molar ratio of 22%, respectively, are illustrated in Fig. 2. The melting

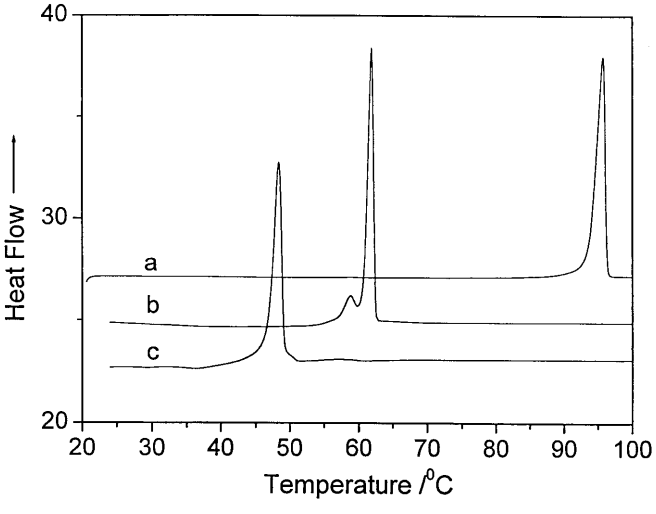

Fig. 2 DSC curves of *a* the PEO–*p*-dibromobenzene (*PDBB*) intercalate with a PDBB molar ratio of 23%, *b* pure PEO and *c* the PEO–PBT intercalate with a PBT molar ratio of 22%

curve of the PEO–PDBB intercalate given in Fig. 2, curve a shows one sharp endothermic melting peak at 95 °C, which is approximately in agreement with the data reported by Point et al. [9]. The DSC trace of the PEO–PBT intercalate with a PBT molar ratio of 22% presents only one sharp peak at 48.5 °C and no eutectic endotherm is observed in the range from 20 to 70 °C (Fig. 2, curve c). It also validates that the stoichiometry of the PEO–PBT intercalate is 22%. Melting double peaks are observed on heating pure PEO (Fig. 2, curve b). The main peak at 62 °C and the small one at 59 °C are attributed to the melting of extended-chain PEO crystals and that of crystals once folded, respectively [13]. Interestingly, the melting curves of the PEO–PBT intercalate and the PEO–PDBB intercalate do not exhibit double peaks like pure PEO even if the PEO–PD*X* intercalate is believed to consist of extended-chain crystals and crystals once folded [8]. A possible explanation is that DSC cannot distinguish the melting of extended-chain crystals from that of folded crystals for these intercalates. Unlike the PEO–PDBB intercalate, the PEO–PBT intercalate has a lower melting point than pure PEO, indicating the very weak interaction between PEO and PBT molecules. As is known, PEO chains adopt an adjacent reentry and deposit in quasi-independent layers during the crystallization. The layered morphology of PEO crystals allows some small guest molecules with specific size and shape to intercalate between adjacent layers. Because of the very weak van der Waals interaction between PBT and PEO molecules, the intercalation of PBT molecules impairs the association of adjacent layers of PEO packing chains and makes the crystal lattices weaker. In contrast, because of the relatively strong van der Waals interactions in the PEO–PDBB intercalate, the intercalation of PDBB molecules reinforces the association of adjacent layers of PEO packing chains and makes the crystal lattices more solid. As a result, the melting point of the PEO–PBT intercalate reduces to 48.5 °C, compared with 62 °C for pure PEO, but rises to 95° C for the PEO–PDBB intercalate.

The powder WAXD spectra for pure PEO, pure PBT and the PEO–PBT intercalate at different temperatures are illustrated in Fig. 3. The spectrum in Fig. 3, curve a for pure PEO at room temperature has diffraction peaks at $2\theta = 18.9°$ ($d = 4.70$ Å), 23.0° ($d = 3.86$ Å), 25.9° ($d = 3.43$ Å) and 26.7° ($d = 3.33$ Å), characteristic of the monoclinic unit cell proposed by Takahashi et al. [14] and Tadokoro et al. [15]. The powder WAXD spectrum in Fig. 3, curve c for the PEO–PBT intercalate at room temperature shows a new diffraction peak at $2\theta = 20.0°$ ($d = 4.43$ Å), which is absent in the WAXD spectra for pure PEO as well as pure PBT (Fig. 3, curve e). In addition, the diffraction peaks observed for the PEO–PBT intercalate occur at $2\theta = 19.1°$, 23.4°, 26.5° and 27.0°, corresponding to the diffraction peaks

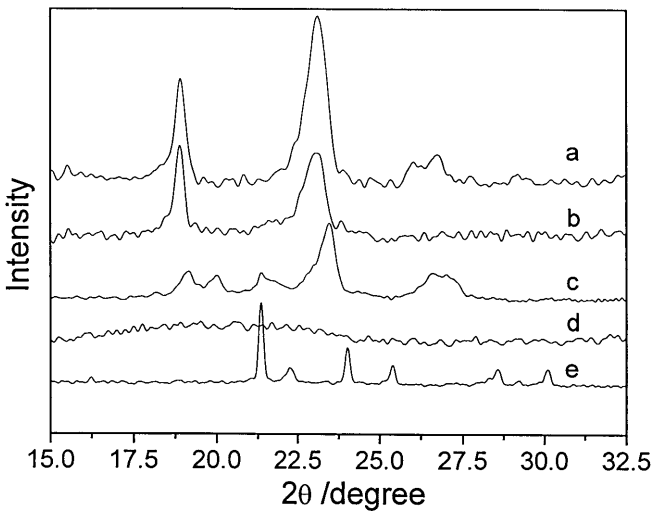

Fig. 3 The powder wide-angle X-ray diffraction spectra of *a* pure PEO at room temperature, *b* pure PEO at 50 °C, *c* the PEO–PBT intercalate at room temperature, d the PEO–PBT intercalate at 50 °C and *e* pure PBT at room temperature

at 18.9°, 23.0°, 25.9° and 26.7° for pure PEO. The WAXD data demonstrate that PEO forms a molecular intercalate with PBT, and the intercalate with a PBT molar fraction of 22% has a new crystalline structure different from that of pure PEO.

The FTIR spectra measured for the PEO–PBT intercalate, pure PEO and PEO–PDBB are exhibited in Fig. 4. Among the IR absorption of pure PEO (Fig. 4, curve b), the band at 1,359 cm^{-1} is mainly caused by the CH_2 symmetric wagging mode, and the band at 1,280 cm^{-1} is associated with the CH_2 asymmetric and symmetric twisting mode. Additionally the band at

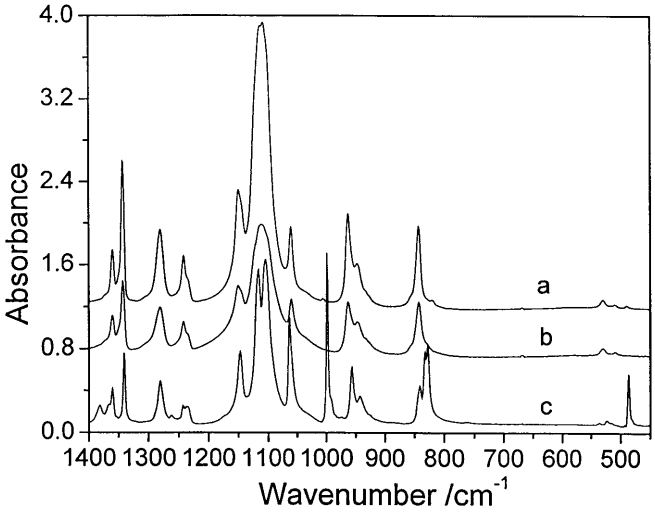

Fig. 4 IR spectra in the range from 1,400 to 450 cm^{-1} for *a* the PEO–PBT intercalate, *b* pure PEO and *c* the PEO–PDBB intercalate

1,060 cm^{-1} is assigned to the COC asymmetric stretching mode coupled with the CH_2 symmetric rocking mode. As to the band at 843 cm^{-1}, it arises from the CH_2 asymmetric rocking mode. These four IR bands have been discussed by several authors in relation to the PEO chain conformation, and are considered to be characteristic of 7/2 helical chains [16, 17, 18]. The IR spectrum of the PEO–PBT intercalate presented in Fig. 4, curve a exactly resembles that of pure PEO; however, it is found that after intercalation the bands at 1,013 cm and 802 cm^{-1} attributed to pure PBT shift to 1,006 cm and 819 cm^{-1}, respectively. This is in accordance with the observation by Point et al. [10]. As to the PEO–PBT intercalate, the conformational regularity bands at 1,359, 1,280, 1,060 and 843 cm^{-1} almost remain unchanged. It implies that the PEO chains in the PEO–PBT intercalate adopt a 7/2 helical conformation identical with that in pure PEO. Figure 4, curve c shows the IR spectrum of the PEO–PDBB intercalate. It can be found that the conformational regularity bands of interest shift slightly to 1,360, 1,281, 1,063 and 840 cm^{-1}, suggesting a variation of the PEO chain conformation in the PEO–PDBB intercalate. This observation further verifies that the PEO chains in the category of PEO–PDX intercalates adopt a 10/3 helical conformation which is considered very close to the 7/2 helical conformation in pure PEO [11].

The difference between the PEO–PBT and PEO–PDBB intercalates in the IR spectra can also be explained on the basis of van der Waals interactions. In the PEO–PBT intercalate, the interaction between PBT molecules and PEO chains is just a very weak physical association, which does not enable the PEO chains to change their own conformations, and the PEO chain conformation remains the 7/2 helix. Consequently, no shift of the aforementioned conformational regularity bands is observed. In the case of the PEO–PDBB intercalate, PDBB molecules interact with PEO chains strongly enough to modify the PEO chain conformation, so the conformation of the PEO chains transforms into a 10/3 helix. This leads to the slight shift of the related conformational regularity bands.

To study further the phase transition and the macromolecular chain conformation, an in situ heating FTIR spectroscopic technique was applied to investigate the variation of the conformational regularity bands with temperature. The IR spectra of the PEO–PBT intercalate with a PBT molar fraction of 22% and pure PEO measured at various temperatures with a heating rate of 5 °C min^{-1} are displayed in Figs. 5 and 6. In both cases, the conformational regularity bands at 1,359, 1,280, 1,060 and 843 cm^{-1} weaken gradually with increasing temperature and disappear at sufficiently high temperature. In the meantime, the two bands at 1,298 cm and 1,250 cm^{-1} (CH_2 twisting) appear during the heating process and increase in intensity with

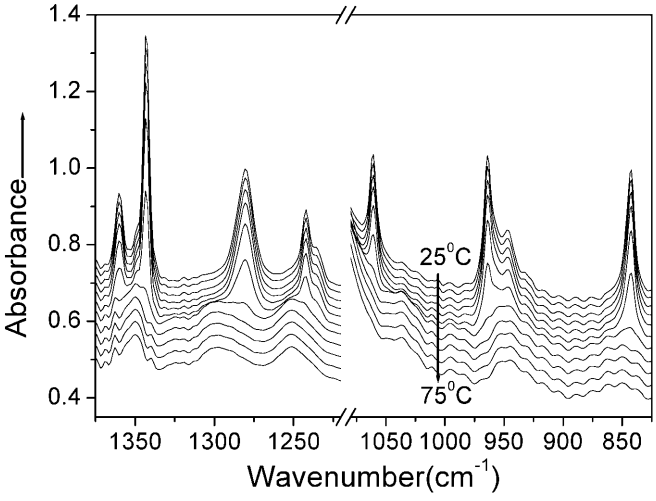

Fig. 5 IR spectra of the PEO–PBT intercalate recorded during heating (5 °C min^{-1}) between 25 and 75 °C

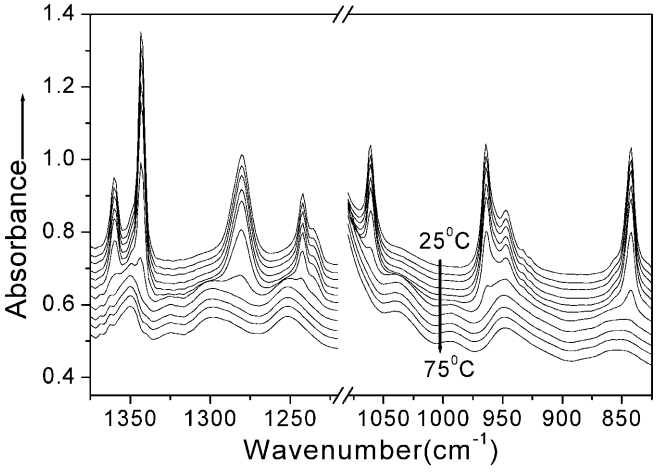

Fig. 6 IR spectra of pure PEO recorded during heating (5 °C min^{-1}) between 25 and 75 °C

increasing temperature. The new bands originate from the conformational disordering of the PEO chains [18]. This indicates that the helical structures in both the PEO–PBT intercalate and pure PEO decrease and the disorder structures increase correspondingly in the process of heating. Since each conformational regularity band has its own absorption, the IR intensities of these bands should be normalized. The variation of the relative intensities versus temperature for all the conformational regularity bands are presented in Fig. 7. By combining Fig. 7 with other experimental data given earlier, further explanation can be made as follows:

1. In the case of pure PEO, the conformational regularity bands at 1,359, 1,280, 1,060 and 843 cm^{-1} almost disappear simultaneously at 60 °C, which

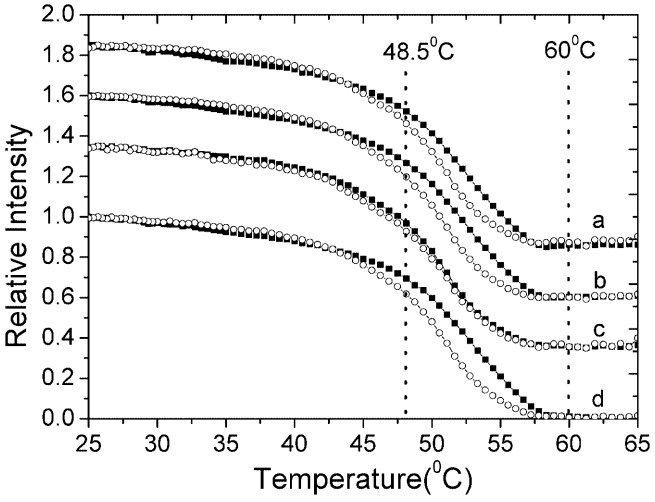

Fig. 7 The variation of the relative intensities of the conformational regularity bands with temperature for pure PEO (*filled symbols*) and for the PEO–PBT intercalate (*open symbols*): *a* 1,359, *b* 1,280, *c* 1,060 and *d* 843 cm^{-1}. The IR intensities of all the bands were normalized to 1. In order to be displayed separately, the curves for the bands at 1,359, 1,280 and 1,060 cm^{-1} were shifted on the *y*-axis

approximately corresponds to the melting point of pure PEO. Thus, the phase-transition information of pure PEO determined from in situ heating FTIR data accords with that obtained from DSC data. Furthermore, it can be inferred that no helical structure exists in the PEO melt when the temperature is higher than 60 °C.

2. For the PEO–PBT system, the phase diagram shows that it undertakes a peritectic reaction at 48.5 °C giving a liquid phase and pure PEO crystals. The PEO–PBT intercalate has a sharp melting endotherm with a peak temperature of 48.5 °C during the heating, which indicates the abrupt collapse of the intercalate crystal lattice at 48.5 °C (Fig. 2, curve c), The powder WAXD spectrum of the PEO–PBT intercalate obtained at 50 °C exhibits no diffraction peak (Fig. 3, curve d), but strong diffraction peaks are retained in the WAXD pattern of pure PEO at 50 °C (Fig. 3, curve b). It demonstrates that the three-dimension crystal lattices of the PEO–PBT intercalate collapse below 50 °C. However, Fig. 7 shows that the intensities of the four aforementioned conformational regularity bands of the PEO–PBT intercalate remain strong at 50 °C. They disappear completely until a temperature of 60 °C is reached. This phenomenon indicates the existence of a considerably large number of helical structures in the melt of the PEO–PBT intercalate over the temperature range from 50 to 60 °C. This IR data can well reflect the incongruent melting behavior of the PEO–PBT intercalate determined by DSC. The conformational order of the PEO–PBT melt containing a remarkable number of helical structures is lower with respect to the crystalline state, but is higher than the unperturbed equilibrium melt [19].
3. The intensity of each conformational band for the PEO–PBT intercalate decreases with increasing temperature slightly faster than that of its corresponding band for the pure PEO, which may be caused by the collapse of the PEO–PBT crystal lattice at lower temperature.

Conclusion

In this work, the phase transition of the PEO–PBT system was determined on the basis of DSC data. The PEO–PBT phase diagram is characteristic of a peritectic system, which exhibits incongruent melting at 48.5 °C and eutectic melting at 24 °C. The molar stoichiometry of the PEO–PBT intercalate is found to be 22%. The incongruent melting point of 48.5 °C for the PEO–PBT intercalate is lower than the melting point of pure PEO and that of the PEO–PDBB intercalate. This may be due to the very weak van der Waals interactions between the PBT and PEO molecules. The WAXD spectrum of the PEO–PBT intercalate exhibits a new diffraction peak at $2\theta = 20.0°$ ($d = 4.43$Å), which is absent in the spectra of pure PEO and PBT. Additionally, the diffraction peaks of the PEO–PBT intercalate are located at $2\theta = 19.1°$, 23.4°, 26.5° and 27.0°, corresponding to those observed for pure PEO at 18.9°, 23.0°, 25.9° and 26.7°, respectively. This suggests that the PEO–PBT intercalate has a crystalline structure quite different from that of pure PEO.

The IR spectrum of the PEO–PBT intercalate exactly resembles that of pure PEO, and the conformational regularity bands at 1,359, 1,280, 1,060 and 843 cm^{-1} remain almost unchanged after intercalation. It is considered that the chain conformation in the PEO–PBT intercalate is the same as the 7/2 helical conformation in pure PEO. Coupled with WAXD, in situ heating FTIR spectroscopy was employed to investigate the phase transition and chain conformation for the PEO–PBT intercalate. It is found that a large number of helical structures exist in the melt of the PEO–PBT intercalate at 50 °C despite the complete collapse of the three-dimension crystal lattice. These helical structures exist until the temperature rises to 60 °C. These IR results fit well to the incongruent melting behavior determined by the DSC measurements. The melt of the PEO–PBT intercalate at temperatures ranging from 50 to 60 °C is in a high-order state because it contains a lot of 7/2 helical structures.

Acknowledgements This work was subsidized by Bruker Co., the National Natural Science Foundation of China NNSFC No. 20104004 and the Special Funds for Major State Basic Research Projects (G1999064802).

References

1. Iwamoto R, Saito Y, Ishihara H, Tadokoro H (1968) J Polym Sci A2 1509
2. Chatani Y, Okamura S (1987) Polymer 28:1815
3. Tadokoro H, Yoshihara T, Chatani Y, Murahashi S (1964) J Polym Sci B2 363
4. Myasnikiova RM, Titova EF, Obolonkova ES (1980) Polymer 21:403
5. Delaite E, Point JJ, Damman P, Dosière M (1992) Macromoleules 25:4768
6. Point JJ, Damman P (1992) Macromolecules 25:1184
7. Paternostre L, Damman P, Dosière M (1999) J Polym Sci Part B Polym Phys 37:1197
8. Paternostre L, Damman P, Dosière M (1998) Polymer 39:4579
9. Point JJ, Coutelier C (1985) J Polym Sci Part B Polym Phys 23:231
10. Point JJ, Jasse B, Dosière M (1986) J Phys Chem 90:3273
11. Point JJ, Coutelier C, Villers D (1986) J Phys Chem 90:3277
12. Angood AC, Koenig JL (1968) J Appl Phys 39:4985
13. Delaite E, Point JJ, Damman P, Dosière M (1992) Macromolecules 25:4768
14. Takahashi Y, Tadokoro H (1973) Macromolecules 6:359
15. Tadokoro H, Chatani Y, Yoshihara T, Tahara S, Murahashi S (1964) Makromol Chem 73:109
16. Krimm S (1960) J Chem Phys 32:1780
17. Yoshihara T, Tadokoro H, Murahashi S (1964) J Chem Phys 41:2902
18. Guo C, Liu H, Wang J, Chen J (1999) J Colloid Interface Sci 209:368
19. Zhu X, Yan D, Yao H, Zhu P (2000) Macromol Rapid Commun 21:354